12. G. Z. Gershuni and E. M. Zhukhovitskii, Convective Stability of an Incompressible Fluid [in Russian], Moscow (1972).
13. N. N. Bogolyubov and Yu. A. Mitropol'skii, Asymptotic Methods in the Theory of Nonlinear Oscillations, Hindustan Publ. Co. (1963).
14. R. V. Khokhlov, Dokl. Akad. Nauk SSSR, 97, No. 3, 411-414 (1954).
15. C. Hayashi, Nonlinear Oscillations in Physical Systems, McGraw-Hill, New York (1964).

NONSTATIONARY PROCESSES IN OPTICAL FIBER FORMATION.

1. STABILITY OF THE DRAWING PROCESS

V. N. Vasil'ev, G. N. Dul'nev, and V. D. Naumchik

UDC 532.51:532.522

The stability of quartz glass melt flow in the deformation domain is investigated in the linear hydrodynamic stability approximation as a function of the velocity coefficient, the drawing rate, and the temperature modes of optical fiber formation.

One of the fundamental quality indices of an optical fiber is the constancy of its geometric dimensions along the length. Fluctuations of the lightguide diameter cause nonstationary processes during its formation, for instance, fluctuations of the melt viscosity in the deformation zone, small fluctuations of the feeding and drawing velocities, inhomogeneity of the ingot, etc. Since different perturbations are inevitably present in any real process of optical fiber fabrication, the sensitivity of the lightguide dimensions to small fluctuations in the drawing parameters near their stationary values is of great interest. Closely related to the problem of investigating the reaction of the optical fiber drawing process to external perturbing effects is the problem of its stability because it governs the domain of the parameters where continuous fiber formation is possible.

Instability of the process can be caused by two mechanisms: cohesion breakaway of the lightguide (the tensile stress exceeds its rupture strength), and hydrodynamic instability (small perturbations increase without limit in time and cause fracture of the liquid jet or a periodic change in the thickness of the fiber being formed appears, i.e., so-called drawing resonance is observed). The first fracture mechanism during the drawing of quartz lightguides is associated with underheating of the quartz glass melt, i.e., with too high a value of the viscous friction and is not examined here.

Investigation of the stability of the fiber formation process was performed first for the case of drawing from a filler of a continuous polymeric or vitreous textile fiber in isothermal [1, 2] and nonisothermal conditions [3-5]. However, the application of these results directly to production of optical fiber is difficult (the isothermal model is too rough a generalization and mainly fiber drawing of polymers was examined in [3-5] and the energy equation being used cannot adequately describe the heat transfer process in lightguide production). The stability of optical fiber drawing was studied directly in [6-9] but the stability was investigated in [6-8] only within the framework of the hydrodynamic model. The ingot heating conditions were not examined here while the temperature distribution in the equations of motion was taken into account parametrically by giving the viscosity by a function of the longitudinal coordinate. The system of governing equations in [9] is actually borrowed completely from [3, 5], therefore, the remark formulated above relative to [3, 5] also refers to [9]. Let us note that the dependence of the drawing stability on the temperature conditions for fiber formation is shown convincingly in [8, 9]. It follows from the survey presented that the drawing stability problem for optical lightguides is insufficiently investigated. For a correct solution of the problem posed the heat exchange process during fiber production must be examined more completely since it is apparently governing.

1. Stability of the optical fiber drawing process is investigated in this paper within the framework of the linear theory of stability on the basis of a quasi-one-dimensional model [10]. Fiber formation is considered under simple uniaxial tension of a Newtonian fluid with

Leningrad Institute of Precision Mechanics and Optics. Translated from Inzhenerno-Fizicheskii Zhurnal, Vol. 55, No. 2, pp. 284-292, August, 1988. Original article submitted March 17, 1987.

 0022-0841/88/5502-0918$12.50

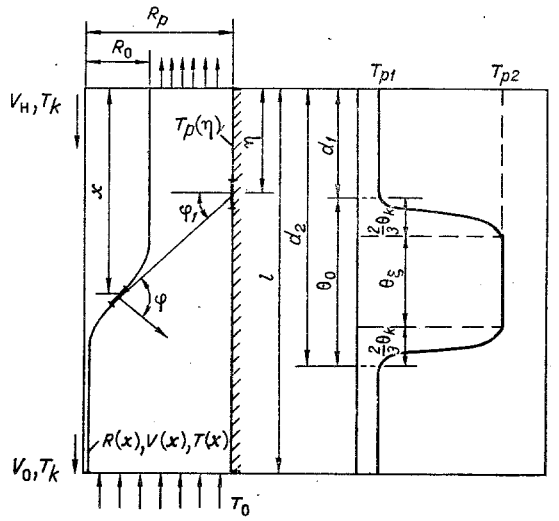

Fig. 1. Configuration of the computation domain.

variable viscosity governed by the temperature distribution. It is assumed in the derivation of the continuity, motion, and energy equations that the physical properties of glass, with the exception of viscosity, are constant, the liquid is isotropic and its motion is axisymmetric. The heat conductivity equation is written for the case of ingot heating in a furnace (Fig. 1). The system of governing equations is written as follows in dimensionless form [10]:

$$-\frac{\partial R}{\partial \tau} = V\frac{\partial R}{\partial x} + \frac{R}{2}\frac{\partial V}{\partial x}, \tag{1}$$

$$R^2\left(\frac{\partial V}{\partial \tau} + V\frac{\partial V}{\partial x}\right) = \frac{1}{\mathrm{Re}}\frac{\partial}{\partial x}\left(3\mu R^2\frac{\partial V}{\partial x}\right) + \frac{R^2}{\mathrm{Fr}} + \frac{1}{\mathrm{We}}\frac{\partial R}{\partial x}, \tag{2}$$

$$R^2\left(\frac{\partial T}{\partial \tau} + V\frac{\partial T}{\partial x}\right) = \frac{1}{\mathrm{Pe}}\frac{\partial}{\partial x}\left(\lambda R^2\frac{\partial T}{\partial x}\right) - 2R(1+R'^2)^{1/2}\mathrm{St}(T-1) + \tag{3}$$

$$+ 4\chi R R_p(R_p - R)\int_0^1 \frac{(\beta\varepsilon_p T_p^4 - \varepsilon T^4)[R_p - R + kR'(x-\eta)]}{[(\eta-x)^2 + (R_p-R)^2]^2}\,d\eta,$$

where $\bar{V} = V/V_0$, $\bar{\mu} = \mu/\mu_0$, for the geometric parameters $\bar{y} = y/l$ ($y \in \{x, R, l, R_p, R_0\}$), for the temperature $\bar{t} = t/T_0$ ($t \in \{T_0, T, T_p, T_k\}$), $\bar{\lambda} = \lambda_e/\lambda_T$, $\bar{\tau} = \tau V_0/l$, $\mathrm{Pe} = \rho V_0 c l/\lambda_T$, $\mathrm{Re} = \rho V_0 l/\mu_0$, $\mathrm{St} = h/\rho V_0 l$, $\chi = n_c^2\sigma_0 T_0^3/c\rho V_0$, $\mathrm{We} = V_0\rho l/\sigma$, $\mathrm{Fr} = 2V_0^2/gl$, and k is a weight factor,

$$k = \begin{cases} -1, & \text{if } R' > 0, \\ 1, & \text{if } R' < 0, \end{cases} \quad R' = \partial R/\partial x.$$

The bar above the dimensionless variables is omitted in writing (1)-(3) while the temperature dependence of the viscosity was modeled by the following relationships: $\mu(T) = \mu_0\exp(-\bar{a}_2 T + a_1)$ [11].

Let us form the equation describing the perturbation of the stationary state of the drawing mode. When investigating the Laminar flow stability its governing parameters are decomposed into fundamental and perturbing which are superposed on the fundamental. Let $V(x)$, $T(x)$, $R(x)$ be the velocity, temperature distribution, and shape of the jet surface for the steady state while $\tilde{V}(x,\tau)$, $\tilde{T}(x,\tau)$, $\tilde{R}(x,\tau)$ characterize the perturbation of the stationary state dependent on not only the coordinate x but also on the time. Then the governing parameters of of the resultant state can be written in the following form

$$\bar{\bar{V}}(x,\tau) = V(x)[1+\tilde{V}(x,\tau)],\ \bar{\bar{T}}(x,\tau) = T(x)[1+\tilde{T}(x,\tau)],$$
$$\bar{\bar{R}}(x,\tau) = R(x)[1+\tilde{R}(x,\tau)]. \tag{4}$$

TABLE 1. Dependence of the Accuracy of Determining ω_1^1 on the Discretization of the Design Domain

N	W	ω_i^1	Critical value W	N	W	ω_i^1	Crical value W
40	15	—0,787	Not fixed	60	15	—0,372	21,38
	30	—0,461			30	0,256	
	70	—0,121			70	0,767	
50	15	—0,653	36,71	70	15	—0,322	20,37
	30	—0,107			30	0,264	
	70	0,184			70	0,987	

The stability investigation problem is to clarify whether the perturbing action damps out or grows in time for a given fundamental flow. Let us substitute (4) into (1)-(3), and after linearizing with respect to the variables $\tilde{V}$, $\tilde{T}$, $\tilde{R}$ with the parameters of the fundamental flow, i.e., the functions R(x), V(x), T(x), satisfying equations (1)-(3) for the steady state taken into account, we obtain a system of differential equations describing the perturbation of the stationary drawing mode:

$$-\frac{\partial\tilde{R}}{\partial\tau}=V\frac{\partial\tilde{R}}{\partial x}+\frac{R}{2}\frac{\partial\tilde{V}}{\partial x}, \tag{5}$$

$$\frac{\partial\tilde{V}}{\partial\tau}=\frac{3\mu}{\mathrm{Re}}\frac{\partial^2\tilde{V}}{\partial x^2}+\beta_1(x)\frac{\partial\tilde{V}}{\partial x}+\beta_2(x)\tilde{V}+\alpha_1(x)\frac{\partial\tilde{R}}{\partial x}+\alpha_2(x)\tilde{R}+\varphi_1(x)\frac{\partial\tilde{T}}{\partial x}+\varphi_2(x)\tilde{T}, \tag{6}$$

$$\frac{\partial\tilde{T}}{\partial\tau}=\frac{\lambda}{\mathrm{Pe}}\frac{\partial^2\tilde{T}}{\partial x^2}+\varphi_3(x)\frac{\partial\tilde{T}}{\partial x}+\varphi_4(x)\tilde{T}+\alpha_3\frac{\partial\tilde{R}}{\partial x}+\alpha_4(x)\tilde{R}+\beta_3(x)\tilde{V}, \tag{7}$$

where

$$\beta_1(x)=\frac{3}{\mathrm{Re}}\left[\frac{2(\mu RV)'}{RV}-\mu'\right]-V,\ \beta_2(x)=\frac{1}{R^2V\,\mathrm{Re}}\frac{d}{dx}\left(3\mu R^2\frac{dV}{dx}\right)-2V',$$

$$\beta_3(x)=-\frac{VT'}{T},\ \alpha_1(x)=\frac{6\mu V'}{V\,\mathrm{Re}}-\frac{1}{RV\,\mathrm{We}},\qquad \alpha_2(x)=\frac{2}{R^2V\,\mathrm{Re}}\frac{d}{dx}\left(3\mu R^2\frac{dV}{dx}\right)+\frac{R'}{R^2V\,\mathrm{We}},$$

$$\alpha_3(x)=\frac{2\lambda T'}{T\,\mathrm{Pe}}-\frac{2R'\,\mathrm{St}}{T}(T-1)+\frac{4\chi kR_p(R_p-R)}{T}\int_0^1\frac{(\beta\varepsilon_pT_p^4-\varepsilon T^4)(x-\eta)}{[(\eta-x)^2+(R_p-R)^2]^2}d\eta,$$

$$\alpha_4(x)=\frac{2}{R^2T\,\mathrm{Pe}}\frac{d}{dx}\left(\lambda R^2\frac{dT}{dx}\right)-\frac{2(1+3/2R'^2)\,\mathrm{St}}{RT}(T-1)-\frac{2VT'}{T}+$$

$$+\frac{4\chi R_p}{RT}\int_0^1(\beta\varepsilon_pT_p^4-\varepsilon T^4)\left\{\frac{(R_p-R)(R_p-3R)+kR'(x-\eta)(2R_p-3R)}{[(\eta-x)^2+(R_p-R)^2]^2}+\frac{4R(R_p-R)^2[R_p-R+kR'(x-\eta)]}{[(\eta-x)^2+(R_p-R)^2]^2}\right\}d\eta,$$

$$\varphi_1(x)=-\frac{3a_2\mu TV'}{\mathrm{Re}\,V},\ \varphi_2(x)=\frac{1}{\mathrm{Re}\,V}\left[3\mu'V'-\frac{a_2T}{R^2}\frac{d}{dx}\left(3\mu R^2\frac{dV}{dx}\right)\right],$$

$$\varphi_3(x)=\frac{2(\lambda RT)'}{RT\,\mathrm{Pe}}-V-\frac{\lambda'}{\mathrm{Pe}},\ \varphi_4(x)=\frac{1}{R^2T\,\mathrm{Pe}}\frac{d}{dx}\left(\lambda R^2\frac{dT}{dx}\right)-$$

$$-\frac{2(1+R'^2)^{1/2}\mathrm{St}}{R}-\frac{VT'}{T}-\frac{16\chi R_p\varepsilon(R_p-R)T^3}{R}\int_0^1\frac{R_p-R+kR'(x-\eta)}{[(\eta-x)^2+(R_p-R)^2]^2}d\eta.$$

Here $(\ldots)' = d/dx$, $a_2 = \bar{a}_2T_0$, and the coefficients $\beta_i(x)$, $\alpha_i(x)$, $\varphi_i(x)$ are evaluated in terms of the functions R(x), V(x), T(x) which are solutions of the system (1)-(3) for the steady state under the following boundary conditions

$$R=R_0,\ V=V_{\mathrm{H}},\ T=T_k\ \text{ for }\ x=0, \tag{8}$$

$$V = 1, \quad \frac{\partial T}{\partial x} = 0 \quad \text{for} \quad x = 1, \tag{9}$$

where V_H is the dimensionless rate of ingot delivery, T_k is the dimensionless temperature on the boundaries of the design domain, and R_0 is the dimensionless ingot radius.

We seek the solution of the system (5)-(7) in the form

$$\tilde{\Psi}(x, \tau) = \psi(x) e^{-i\omega\tau}, \tag{10}$$

since any perturbation can be expanded in a Fourier series and represented as the sum of separate fluctuations of the form (10). Here $\psi(x) = \psi(x) + i\tilde{\psi}(x)$ is the complex amplitude and $\omega = \omega_2 + i\omega_1$, where ω_1 is the growth coefficient, i.e., the quantity permitting a judgment as to whether the fluctuation $\tilde{\Psi}(x, \tau)$ ($\tilde{\Psi}(x, \tau) \in \{\tilde{R}(x, \tau), \tilde{V}(x, \tau), \tilde{T}(x, \tau)\}$, $\psi(x) \in \{r(x), v(x), t(x)\}$) grows or damps out.

Substituting (10) into (5)-(7), we obtain a system of ordinary differential equations to determine $\Psi(x)$ and ω of the following form

$$Vr' + \frac{R}{2} v' + i\omega r = 0, \tag{11}$$

$$\frac{3\mu}{\mathrm{Re}} v'' + \beta_1(x) v' + [\beta_2(x) + i\omega] v + \alpha_1(x) r' + \alpha_2(x) r + \varphi_1(x) t' + \varphi_2(x) t = 0, \tag{12}$$

$$\frac{\lambda}{\mathrm{Pe}} t'' + \varphi_3(x) t' + [\varphi_4(x) + i\omega] t + \alpha_3(x) r' + \alpha_4(x) r + \beta_3 V = 0. \tag{13}$$

Here $(\ldots)'' = d^2/dx^2$, $(\ldots)' = d/dx$. The boundary conditions for (11)-(13) are obtained from (8) and (9) after successive substitution of (4) and (10) therein:

$$r(0) = v(0) = t(0) = 0, \quad v(1) = t'(1) = 0. \tag{14}$$

Therefore, investigation of the stability of the optical fiber drawing process is an eigenvalue problem for the system of ordinary differential equations (11)-(13) under the boundary conditions (14). Corresponding to each eigenvalue ω_i^j will be a mode of the form $\tilde{\Psi}^j(x,\tau) = [\Psi^j(x) + i\tilde{\Psi}^j(x)] e^{-\omega_r^j \tau} e^{-\omega_i^j \tau}$. The quantity ω_i^j determines either the growth ($\omega_i^j > 0$) or damping ($\omega_i^j < 0$) of the perturbation by its sign, i.e., for $\omega_1^j < 0$ the given flow $\{R(x), V(x), T(x)\}$ for a given perturbation $\tilde{\Psi}^j(x, \tau)$ is stable while for $\omega_1^j > 0$ it is unstable.

If a finite-difference method is used, then the system of differential equations (11)-(13) with the boundary conditions (14) can be compared to a system of linear homogeneous algebraic equations of the form

$$(iA - \omega E) X = 0, \tag{15}$$

where E is the unit matrix, $X = (\ldots, r_k, v_k, t_k, \ldots)^T$, A is a tape matrix obtained as a result of approximating (11)-(13) by finite difference relationships, and $\psi'' = (\psi_{k+1} - 2\psi_k + \psi_{k-1})/\xi^2$, $\psi' = (\psi_k - \psi_{k-1})/\xi$. A nontrivial solution of the homogeneous system of equations (15) exists if and only if

$$\det(iA - \omega E) = 0. \tag{16}$$

Therefore, the finite-difference method permits reduction of the eigenvalue problem for the system of differential equations to an algebraic eigenvalue problem (16). The initial complex matrix of the system (15) for the numerical computations was reduced by unitary transformations to the upper Hessenberg form which was then used to calculate all the eigenvalues by the QR-algorithm with a shift [12].

2. As the first step in the numerical investigation of the optical fiber drawing process within the framework of the approach elucidated, we consider lightguide formation with a constant temperature distribution in the deformation zone (isothermal drawing). For this case the system of equations describing the perturbed state consists of the equation (the analog of (12) for the isothermal mode)

$$\frac{3}{\mathrm{Re}}v''+\frac{6(RV)'}{RV\,\mathrm{Re}}v'+\left[\frac{3}{R^2V\,\mathrm{Re}}\frac{d}{dx}\left(R^2\frac{dV}{dx}\right)-2V'-i\omega\right]v+$$
$$+\left(\frac{6V'}{\mathrm{Re}\,V}+\frac{1}{RV\,\mathrm{We}}\right)r'+\left[\frac{6}{R^2V\,\mathrm{Re}}\frac{d}{dx}\left(R^2\frac{dV}{dx}\right)+\frac{R'}{R^2V\,\mathrm{We}}+\frac{2}{V\,\mathrm{Fr}}-2V'\right]r=0 \qquad (17)$$

and (11), while the stationary fiber configurations and the velocity distribution for the calculation of the coefficients in (11) and (17) are found from the stationary solution of (1) and (2) for $\mu = \mathrm{const}$.

Analogously to the above consideration the stability investigation problem for isothermal drawing was reduced to an algebraic eigenvalue problem. The difficulty with the finite-difference approach is mainly that the accuracy of finding the critical value of the velocity coefficient $W = V_0/V_H$ is determined by discretization of the design domain. Presented in Table 1 are values of the magnitude of the damping factor for the first mode (it is considered that the first mode has the maximal value of ω_1^j) as a function of W and N. The most satisfactory results are obtained for $50 < N < 70$, consequently, in all the subsequent computations to determine the critical value of the velocity coefficient its magnitude was found for $N = 50, 60, 70$ with subsequent extrapolation to $1/N \to 0$ since the error in determining W_{cr} is proportional to 1/N. For the case presented in Table 1 (melt temperature 2000°C), $E_{cr} = 20.28$, which is in good enough agreement with the data of previous investigations [8].

The quantity W_{cr} was used in [1, 2, 8] as the criterion characterizing melt flow stability in isothermal fiber drawing. It was considered that for $W > W_{cr}$ the flow is unstable for all drawing modes, and conversely, is stable for $W < W_{cr}$. Computations performed show that a dependence exists between the critical value of the velocity coefficient and the melt temperature in the deformation and drawing velocity zone. It is seen from Table 2 that a temperature rise in the glass mass (within definite limits) or in the drawing velocity (in both cases this is equivalent to increasing the number Re since a diminution in the viscosity occurs in the second case as the temperature rises) for a fixed W results in an increase in the stability of the drawing process. This latter means that it is apparently necessary to use the number Re jointly with W for the characteristics of stability threshold of the melt flow.

3. The stability of a nonisothermal optical fiber drawing process was studied as a function of W and the temperature conditions for fiber formation (the number St and the temperature of the heating element). The temperature distribution along the heating element surface (the function $T_p(\eta)$ in (3)) was modelled by the following relationship (see Fig. 1)

$$T_p(\theta)=\begin{cases} T_{p1},\ -a_1<\theta<0,\ (d_2-d_1)<\theta<(l-d_1), \\ T_{p1}+(T_{p2}-T_{p1})\,6{,}75\,\dfrac{\theta^2(\theta_k-\theta)}{\theta_k^3},\ 0<\theta<\dfrac{2}{3}\theta_k, \\ T_{p2},\ \dfrac{2}{3}\theta_k<\theta<\theta_0-\dfrac{2}{3}\theta_k, \\ T_{p1}+(T_{p2}-T_{p1})\,6{,}75\,\dfrac{(\theta_0-\theta)^2(\theta_k+\theta-\theta_0)}{\theta_k^3},\ \theta_0-\dfrac{2}{3}\theta_k\leqslant\theta\leqslant\theta_0, \end{cases} \qquad (18)$$

TABLE 2. Dependence of the Damping Factor of the First Mode on the Melt Temperature in the Deformation Zone and the Drawing Velocity for W = 20.3

T, (°C)	V_0, m/sec	ω_i^1	T, (°C)	V_0, m/sec	ω_i^1
1900	0,5	0,0319	2250	0,5	—0,0017
	2	—0,8322		2	—0,8456
	5	—2,9621		5	—2,9720
	10	—7,1883		10	—7,1083
2100	0,5	—0,0008	2400	0,5	—0,0057
	2	—0,8347		2	—0,8227
	5	—2,9795		5	—2,9335
	10	—7.1863		10	—6.1289

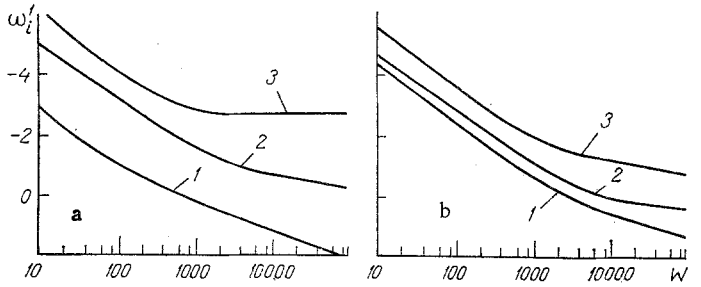

Fig. 2. Dependence of the damping factor of the first mode on W (T_{p1} = 1500°C; T_{p2} = 2200°C, V_0 = 1 m/sec); a) ξ = 0.375, St = 0.05 (1); 0.25 (2); 0.5 (3); b) St = 0.25, ξ = 0.075 (1); 0.75 (2); 0.6 (3).

where $\theta_0 = d_2 - d_1$, $\theta = \eta - d_1$, $\frac{\theta_k}{\theta_\xi} = \xi$, $0.075 \leqslant \xi \leqslant 0.75$. The dependence (18) permits a sufficiently good approximation of the temperature distribution along the heating element surface since it assumes the existence of a kernel θ_ξ with constant temperature and gradient part of the profile (near the boundary surfaces) in the temperature profile, where the temperature varies according to a third degree parabola law. Variation by the quantities T_{p1}, T_{p2}, the dimension of the central section (θ_ξ depends on the constant ξ and for ξ = 0.75 we have θ_ξ = 0 while for ξ = 0.075 $\theta_\xi = 0.9l$) and the length of the heated section (it is governed by the difference $d_2 - d_1$) permits a change in the shape of the temperature distribution along the heating element surface and thereby permits modelling different thermal modes of fiber drawing.

It is seen from Fig. 2 that as W increases for a fixed value of the number St the stability of the drawing process drops (Fig. 2b), while it also depends substantially on the thermal mode of furnace operation (Fig. 2a). The drawing process possesses the least stability for either a low value of the number St (curve 1, Fig. 2b), or for a practically constant heating element surface temperature (curve 1, Fig. 2a which corresponds to the furnace operating mode for a $0.9l$ dimension of the kernel with constant temperature). This latter is explained by the fact that under given conditions the drawing process shifts substantially toward isothermy. Figure 2a also graphically illustrates that for an arbitrary fixed value of the number St a certain optimal temperature mode of heating element operation exists from the viewpoint of the optical fiber drawing process stability. For this case, the condition corresponding to curve 3 in Fig. 2a (the magnitude of the kernel with the constant temperature equals $0.2l$) is most optimal. A less stable mode of fiber formation is formed upon narrowing the heating zone further (curve 2 in Fig. 2a, no kernel with a constant temperature). The appearance of instability in this case is apparently associated with underheating of the glass mass and significant growth of the tensile force when small fluctuations in the technological process parameters result in substantial fluctuations of the tensile force. Analogously to the isothermal case, optical fiber drawing under nonisothermal conditions is marked by the growth in the first mode damping factor as the drawing velocity increases for a fixed value of W (T_{p1} = 1500°C, T_{p2} = 2200°C, ξ = 0.375, W = 77, α = 50 W/(m^2•K)): for V_0 = 1; 5; 10 m/sec ω_i' = −0.976; −5.861; −9.899 respectively.

In conclusion, it must be emphasized that the stability investigation performed for the optical fiber drawing process in both isothermal (see Table 2) and nonisothermal conditions (see Fig. 2) showed that for each mode of fiber formation a dependence of this characteristic of the technological process on the drawing temperature conditions exists. In each specific case a certain interval in the temperature can be extracted in which an increase in stability is first observed as the temperature rises from the lower to the upper boundary with a subsequent diminution as the upper boundary is approached. The lower boundary is determined by the cohesion stability of the drawing process (the magnitude of the tensile force should be less than the fiber strength limit) and the upper by the capillary instability associated with heating the glass mass and by the low value of the viscosity at which dissociation of the liquid jet into drops occurs under the effect of surface tension forces. Therefore, for any fixed value of W, the drawing velocity, certain optimal temperature conditions exist for fiber formation for which the process is maximally stable.

NOTATION

R, R_p, R_0, radii of the deformation, ingot, and heating element zones; τ, time; μ, μ_0, melt viscosity and the viscosity scale when going over to dimensionless variables; x, longitudinal coordinate; T, T_0, T_p, temperatures of the melt, the gas being blown through the heating zone, and the furnace; T_{p1}, T_{p2}, maximal and minimal heating element temperature; λ_r, λ_e, melt and effective coefficient of molecular conductivity which takes account of both the molecular and the radiant conduction; β, reflection coefficient; ε_p, ε, emissivities of the heating element and the melt; η, an integration variable; l, heating element length; ρ, c, melt density and specific heat; h, coefficient of external heat elimination; n_c, refractive index of the gas being blown through the heating zone; σ_0, Stefan–Boltzmann constant; σ, coefficient of surface tension; d_1, d_2, coefficients in the temperature dependence of the viscosity; $\bar{a}_2$, a_1, geometric dimensions of the heating zone; N, quantity of points along the longitudinal coordinate during discretization of the design domain; V, V_H, V_0, velocities of the melt, the ingot delivery, and the drawing.

LITERATURE CITED

1. G. J. Donnelly and C. B. Weinberger, Ind. Eng. Chem. Fund., 14, No. 4, 3-7 (1975).
2. J. R. A. Pearson and Y. T. Shah, Ind. Eng. Chem. Fund., 13, No. 2, 134-138 (1974).
3. Y. T. Shah and J. R. A. Pearson, Ind. Eng. Chem. Fund., 11, No. 2, 150-153 (1972).
4. C. D. Han and R. R. Lamonte, J. Appl. Polym. Sci., 16, 3307-3324 (1972).
5. S. Kase, J. Appl. Polym. Sci., 18, 3279-3304 (1974).
6. F. T. Geyling, BSTJ, 55, No. 8, 1011-1056 (1976).
7. A. L. Yarin, Prikl. Mat. Mekh., 47, No. 1, 86-90 (1983).
8. V. L. Kolpashchikov, Yu. I. Lanin, O. G. Martynenko, and A. I. Shnip, Influence of Drawing Temperature Modes on Stability of Optical Fiber Parameters [in Russian], Preprint, Inst. Heat and Mass Transfer, Beloruss. Acad. Sci., Minsk (1984).
9. F. T. Geyling and G. M. Homsy, Glass Technol., 21, No. 2, 95-102 (1980).
10. V. D. Naumchik, Energy Transfer in Convective Streams [in Russian], Minsk (1985), pp. 64-76.
11. Glicksman, Tr. ASME, Ser. D, 90, No. 3, 28-39 (1968).
12. J. Ortega and W. Pool, Introduction to Numerical Methods of Solving Differential Equations [Russian translation], Moscow (1986).

TEMPERATURE-MEASUREMENT OPTIMIZATION AND NUMERICAL INVERSE CONDUCTION-TREATMENT SOLUTION

E. A. Artyukhin, S. A. Budnik, and A. S. Okhapkin

UDC 536.24

Practical evidence is given that locally optimal measurement planning can be applied in nonstationary thermophysical experiments.

Inverse treatments in thermophysics require a preliminary examination of topics in the formalization and algorithmization, as well as choice of working conditions to provide high accuracy. Simulation results [1] show that the systematic error in solving an inverse treatment is substantially dependent on the number of sensors used in the measurements and the positions of them even if the exact values are known for the measured temperatures. A measurement scheme exists for which one can determine the unknown behavior of the thermophysical characteristics accurately. Measurement plan optimization before the experiments is therefore of interest. One can use experiment planning theory [2].

Optimum temperature-measurement planning is based on the following. We introduce a measurement plan

$$\xi = \{N, \bar{X}\}, \bar{X} = \{X_i\}_1^N.$$

Translated from Inzhenerno-Fizicheskii Zhurnal, Vol. 55, No. 2, pp. 292-299, August, 1988. Original article submitted February 2, 1987.

0022-0841/5502-0924$12.50